*International Journal of Automotive Technology*, Vol. 11, No. 4, pp. 601–610 (2010)
DOI 10.1007/s12239–010–0072–7


1229–9138/2010/053–18

# MODELING, PARAMETER ESTIMATION AND NONLINEAR CONTROL OF AUTOMOTIVE ELECTRONIC THROTTLE USING A RAPID-CONTROL PROTOTYPING TECHNIQUE

R. GREPL[1)*] and B. LEE[2)]

[1)]Mechatronics Laboratory, Faculty of Mechanical Engineering, Brno University of Technology, 616 69 Technicka 2, Brno, Czech Republic
[2)]Department of Mechanical and Automotive Engineering, Keimyung University, Daegu 704-701, Korea

*(Received 23 January 2009; Revised 23 November 2009)*

**ABSTRACT**–An electronic throttle consists of a DC motor, spur gears, a return spring, a position sensor, power electronics and an electronic control unit. Fast and precise position control of this electromechanical system is relatively difficult due to very high friction and the strong nonlinearity of the spring. Simple application of linear control, such as PID, fails. In this paper, two new controller structures suitable for different reference signal types are described. The key component of the position controller is the friction compensator based on either/both feedforward or feedback principles. The quality of the resulting behavior was measured using several criteria including the measure of control activity around the equilibrium position. The control activity directly influences the vibration, the noise and the wear of the servo system. The proposed controllers demonstrated superior behavior compared with other published structures.

**KEY WORDS :** Electronic throttle control, Nonlinear control, Friction compensation, Parameter estimation, Rapid control prototyping

## NOMENCLATURE

| | |
|---|---|
| $\varphi$ | : angle of throttle shaft |
| $\varphi_{\text{ref}}$ | : reference (desired) value of angle |
| $\varphi_{\text{LH}}$ | : LH position of throttle plate |
| $u$ | : control input to throttle, voltage normalized to interval (–1;1) |
| $e$ | : position (angle) error |
| $G$ | : gain limit of derivation |
| $T_s$ | : computation sample time |
| $N$ | : number of sample times |
| $k_P$ | : proportional gain in PID |
| $k_I$ | : integral gain in PID |
| $T_d$ | : derivative time constant in PID |
| $i$ | : electrical current |
| $k_{\text{emf}}$ | : constant of back electromotive force |
| $L$ | : armature inductance |
| $m_e$ | : electrical torque recalculated to throttle shaft |
| $m_M$ | : electrical torque on motor shaft |
| $\tau$ | : mechanical torque |
| $R$ | : armature resistance |
| $i_{12}$ | : total gear ration from motor to throttle shaft |
| $\eta_{12}$ | : total efficiency of mechanical system |
| $k_S$ | : stiffness of the return spring |
| $b_{\text{emf}}$ | : mechanical viscous friction |
| $b$ | : damping of the electromechanical system, which applies to the mechanical viscous damping and the back electromotive force |
| $J_{\text{red}}$ | : mechanical inertial moment reduced to the valve shaft (includes inertia of the DC motor, gearbox, and plate) |
| $J$ | : inertial moment in normalized units |
| $k_{xy}$ | : stiffness of nonlinear spring in given part $xy$ |
| $N$ | : normal force |
| $\mu$ | : dry friction coefficient |
| $p$ | : state value in Reset Integrator model |
| $z$ | : state value in LuGre model |
| $n$ | : nr. of samples for error measurement |
| $d$ | : value of dead zone of the friction compensator |
| $\lambda$ | : parameter of SMC |
| $\alpha$ | : parameter of SMC |
| $T_S$ | : sample time |

*Corresponding author: e-mail: grepl@fme.vutbr.cz

## 1. INTRODUCTION

One important current area of research and development in the automotive industry is focused on the X-by-wire concept. The main idea is adopted from aircraft, where "fly-by-wire" is the standard approach used in military as well as civil aircraft. Computer control has replaced conventional mechanical controls; the actuator is connected to the pilot only by means of a "wire". As a result, the maneu-

verability of the aircraft increases significantly due to computer control of a naturally unstable design. Fly-by-wire is very often mentioned as a typical mechatronic solution.

In automotive design, there are many variants of this philosophy in use already or in development. Examples include steering-by-wire, where conventional mechanical steering is replaced by a sensor and an electrical servo-motor, brake-by-wire, where conventional hydraulic or pneumatic actuators are replaced by electrical ones, and (most commonly) throttle-by-wire, where a sensor and an electrical motor replaces a mechanical linkage between the accelerator pedal and the throttle. (Stence, 2006).

The throttle-by-wire system consists of a pedal sensor, the throttle body (with a DC motor, spur gears and a potentiometer as the position sensor) and an electronic control unit (ECU). Thus, the conventional mechanical linkage of pedal and throttle via a bowden cable is replaced by a mechatronic design.

Full ECU control of throttle plate behavior enables better fuel economy and emissions, and it provides the possibility of using advanced tracking control algorithms or other overall system improvements.

Due to mass production of automotive parts and the corresponding compromises between technical quality and manufacturing costs, high friction is a problem that plagues the throttle mechanism. Moreover, safety regulations require the return of the valve to a slightly open position–a so-called "limp home" (LH) mode–in case of system failure. This feature is implemented by a relatively strong spring near the LH position. However, using this spring stiffness through the full range of the valve would also produce an enormous motor load along with significant energy consumption and heating. In most throttles, a nonlinear spring is used to solve this problem (Pavković *et al*., 2006, Deur *et al*., 2003).

Here, we describe a solution to this problem by illustrating how the advanced control algorithm implemented in the ECU can significantly improve inexpensive electro-mechanical systems.

In the last decade, many authors have published interesting results using electronic throttle control; many of them have been directly related to automotive firms (Pavković *et al*., 2006). The high nonlinearity of the system disqualifies the use of simple linear controls (e.g., PID). It is well known that linear controllers cannot deal with the dry friction phenomenon because steady-state error arises in the case of a PD regulator and oscillations arise in the case of a PID controller.

Figure 1. Photo of an electronic throttle body.

The multi-model approach for throttle modeling has been successfully studied previously (Hadilebbal *et al*., 2007). In this approach, a nonlinear model is replaced by several linear models, and the algorithm switches between them. The work is highly inspired by the PWARX (Piece Wise Auto Regressive eXogenous) method. Other work (Trebi-Ollennu and Dolan, 2004) uses an adaptive fuzzy-control approach applied on unmanned ground vehicles. The whole drive system is modeled and controlled with the goal of low-speed control, and a detailed model of the throttle control is not provided.

Contreras *et al.* have identified throttle parameters (Contreras *et al*., 2002). In their approach, the dynamic friction model of LuGre is used with different inertial reduced moments of mechanical throttles, which are considered in terms of the closing or the opening direction. This model does not discuss its control scheme.

One highly inspiring set of papers has been published by Pavković, Deur, and Vasak (Pavković *et al*., 2006; Deur *et al*., 2003; Vašak *et al*., 2007). In these works, the controller architecture consists mainly of a friction compensator, a LH compensator, and a PID element. There are also other improvements including variable filtering according to the control error, feedforward elements, and gain scheduling of the PID. At a given moment, only one of the friction or LH compensators is used. Deur (Deur *et al*., 2003) describes the self-tuning of compensator parameters. Baotic, a collaborator of Deur, (Baotic *et al*., 2003) uses Model Predictive Control and a Karnopp friction model.

The key issue in effective throttle control is compensation for friction. Because friction is a nonlinear function of velocity, several authors deal with the compensators based on measured or reconstructed velocity (Olsson *et al*., 1998). The authors note that the approach is dependent on the precision of the velocity measurement or estimation. A much better alternative to this approach is the use of position error as the input for the friction compensator (Iserman, 1996; Yang, 2004; Pavković *et al*., 2006; Deur *et al*., 2003).

Sliding Mode Control (SMC) for ETC is also an active area of research. Beghi (Beghi*et al*., 2006) and Zhang *et al*. (2006) use SMC in conjunction with a Sliding Mode Observer and compare it with a Kalman filter.

Also, many researchers use the throttle model as a part of other complex models including the engine, the transmission, the wheels and tires, and the traction control system (Ryu *et al*., 2005; Jung *et al*., 2000; Ishikawa *et al*., 2007).

This paper outlines the authors' development and extension of these cited works in the following ways:

- Development and testing of two new controllers suitable for smooth and staircase signals. Additionally, a feedforward compensation for nonlinear springs was developed, used, and tested; and it proved superior to other published feedback compensation methods.
- Use of multiple-criteria comparisons of different control structures including PID; all controllers were tested using two sample times (minimal and realistic).
- Description of an optimal approach for parameter estimation for the system based on closed-loop data acquisition.

According to other authors, e.g., (Baric*et al*., 2005) and (Pavković, 2006), the air flow over the throttle valve was not included in the experiments and was considered as a disturbance.

The Rapid Control Prototyping (RCP) technique was used with dSpace hardware for maximal time efficiency in the development process.

Preliminary experiments and results which have been further developed and presented in this paper was published by authors in (Grepl and Lee, 2008a) and (Grepl and Lee, 2008b).

## 2. MODEL OF THE ELECTROMECHANICAL THROTTLE

### 2.1. Mechanism and DC Motor

The electromechanical part of the ETC consists of a brushed DC motor, spur gears, a nonlinear return spring, a throttle plate, and a potentiometer (Figure 2). The mechanical equation of motion is of the following form:

$$J_{\text{red}}\ddot{\varphi}=m_{\text{e}}-\tau_{\text{viscous}}-\tau_{\text{spring}}-\tau_{\text{friction}} \tag{1}$$

The expression of electrical equilibrium is the following (using the standard linear model of DC motor):

$$u=Ri+L\frac{\mathrm{d}i}{\mathrm{d}t}+k_{\text{emf}}\dot{\varphi}_{\text{M}} \tag{2}$$

$$m_{\text{M}}=k_{\text{emf}}\,i \tag{3}$$

Gears introduce the following relations between the motor and plate variables:

$$\varphi_{\text{M}}=\varphi i_{12} \tag{4}$$
$$m_{\text{e}}=m_{\text{M}}i_{12}\eta_{12}$$

Usually, one can neglect the dynamics of the electrical part of the DC motor, given by inductance $L$. In this case, the model is static and takes the following form:

$$u=Ri+k_{\text{emf}}i_{12}\varphi$$
$$i=\frac{1}{R}u-\frac{k_{\text{emf}}i_{12}}{R}\dot{\varphi} \tag{5}$$

The expression for electrical torque is the following:

$$m_{\text{e}}=\frac{k_{\text{emf}}i_{12}\eta_{12}}{R}u-\frac{k_{\text{emf}}^2i_{12}^2\eta_{12}}{R}\dot{\varphi} \tag{6}$$

The viscous mechanical torque is of the following form:

$$\tau_{\text{viscous}}=b_{\text{mech}}\dot{\varphi} \tag{7}$$

Next, Equation  can be rewritten as the following:

$$J_{\text{red}}\ddot{\varphi}=\frac{k_{\text{emf}}i_{12}\eta_{12}}{R}u-\frac{k_{\text{emf}}^2i_{12}^2\eta_{12}}{R}\dot{\varphi}-b_{\text{mech}}\dot{\varphi}$$
$$-\tau_{\text{spring}}-\tau_{\text{friction}} \tag{8}$$

$$J_{\text{red}}\ddot{\varphi}=\frac{k_{\text{emf}}i_{12}\eta_{12}}{R}u-\left(b_{\text{mech}}+\frac{k_{\text{emf}}^2i_{12}^2\eta_{12}}{R}\right)\dot{\varphi}$$
$$-\tau_{\text{spring}}-\tau_{\text{friction}} \tag{9}$$

Equation (9) can be divided by $k_{\text{emf}}i_{12}\eta_{12}/R$ to obtain the model in units of voltage:

$$J\ddot{\varphi}=u-b\dot{\varphi}-u_{\text{spring}}(\varphi)-u_{\text{friction}}(\dot{\varphi}) \tag{10}$$

The spring torque applied to the shaft can be generally expressed in the form:

$$\tau_{\text{spring}}=k_S(\varphi)\varphi \tag{11}$$

The stiffness, $k_S$, varies with respect to the throttle position (Figure 3). According to Equation (10), the spring torque in units of voltage, $u_{\text{spring}}(\varphi)$, is used. The stiffness, $k_{\text{HS}}$, expresses the hardstop model stiffness if it is needed to simulate the limitation of plate movement in the model.

For normal throttle operation (within limits), the static spring equation is of the following form:

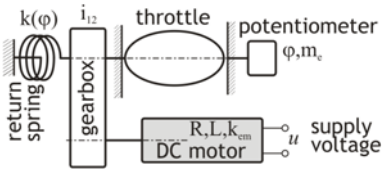


Figure 2. Schematic of the electronic throttle.

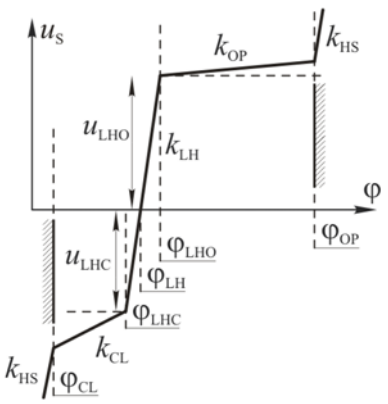


Figure 3. Schema of the nonlinear spring (LH – limp home; CL – throttle closed; OP – throttle opened; HS – the stiffness of hardstops, if modeled).

$$u_S=\begin{cases} k_{LH}(\varphi-\varphi_{LH}), & -u_{LHC}<u_S<u_{LHO} \\ u_{LHO}+k_{OP}(\varphi-\varphi_{LH}), & u_S>u_{LHO} \\ -u_{LHC}+k_{CL}(\varphi-\varphi_{LH}), & u_S>u_{LHO} \end{cases} \quad (12)$$

### 2.2. Friction Models

Usually, the very complex phenomena of friction is considered and modeled as a combination of viscous and dry friction. The viscous component is simple to express, and according to Equation (9), it can be incorporated into the general damping of the electromechanical system, $b$.

Dry friction in the throttle body system is relatively high due to the mass production and consequent low-cost design of the system. The significance of friction is illustrated in Figure 5. Friction accounts for 10% of the input voltage range. The impact of friction on control is even more significant because of the return spring's nature.

The most simple Coulomb friction model,

$$\tau_C(\dot{\varphi})=-\mathrm{sgn}(\dot{\varphi})\mu N, \quad (13)$$

has several well known limitations: a) friction is not defined for zero velocity; b) the model does not cover the increase of friction at near-zero velocities; and c) a non-smooth system is problematic for simulation.

The literature details numerous improvements to the static model, such as including the Stribeck effect, but static friction models are often not sophisticated enough for effective simulation. For this reason, two dynamic friction models are described.

#### 2.2.1. Reset Integrator model

This dynamic friction model effectively describes the stiction effect at near-zero velocities. A new dynamic state, $p$, is considered and can be understood as the bending of a virtual bristle. Proper behavior requires a zero detection feature:

$$\dot{p}=\begin{cases} 0 & \text{if } (v>0\wedge p\geq p_0)\vee(v<0\wedge p\leq -p_0) \\ v & \text{otherwise} \end{cases}$$

$$F_{fric}=\frac{(1+a(p))F_{kin}p}{p_0}+\beta\dot{p} \quad (14)$$

$$a(p)=\begin{cases} a & \text{if } |p|<p_0 \\ 0 & \text{otherwise} \end{cases}$$

This model requires the definition of four parameters: $F_{kin}$ is the kinetic friction; $a$ is the stiction increase of the force in percent (i.e., $a$=0.2 means that the total force when system is sticking is 1.2 $F_{kin}$); $\beta$ is the damping coefficient; and $p_0$ defines the range of stiction.

#### 2.2.2. LuGre model

The LuGre model is the most frequently used dynamic friction model. It has been extensively used in many simulations as well as in practical studies (Olsson *et al.*, 1998). This model is of the following form:

$$\dot{z}=v-\sigma_0\frac{|v|}{g(v)}z$$

$$g(v)=\alpha_0+\alpha_1 e^{-\left(\frac{v}{v_0}\right)^2} \quad (15)$$

$$F_{fric}=\sigma_0 z+\sigma_1\dot{z}+(\alpha_2 v)$$

Thus, it is necessary to estimate five parameters: $\alpha_0$, $\alpha_1$ are kinetic friction and increase of stiction, respectively (see $F_{kin}$ and $a$ in the Reset Integrator model for comparison); $v_0$ is the Stribeck velocity; $\sigma_0$, $\sigma_1$ are the stiffness and damping of "bristles," respectively; and $\alpha_2$ is the normal viscous friction (already included in Equation (9)).

Both dynamic friction models were used in the parameter estimation described in Section 3. The LuGre model better captures system properties, whereas the Reset Integrator is more effective for simulation. This feature can be very important in cases when the throttle model is only one part of a complex model consisting of an engine, a transmission, and/or vehicle dynamics.

## 3. PARAMETER ESTIMATION OF NONLINEAR MODEL

An important class of advanced nonlinear control algorithms (especially friction compensators) requires modeling of the plant (structure, equations) and good estimates of its parameters. This section describes and the search for the parameters (PE, Parameter Estimation) of the aforementioned model.

### 3.1. Initial Experiment Using Open Loop Response

The most important information about the system properties can be obtained using the response to a slow sinusoidal input, $u$. Figure 4 shows the measured current and angle, $\varphi$, in the time domain. Figure 5 shows the $\varphi$–$u$ plot. This experiment confirms the following: a) the stiff nature of the return spring near the LH position, b) the significant fric-

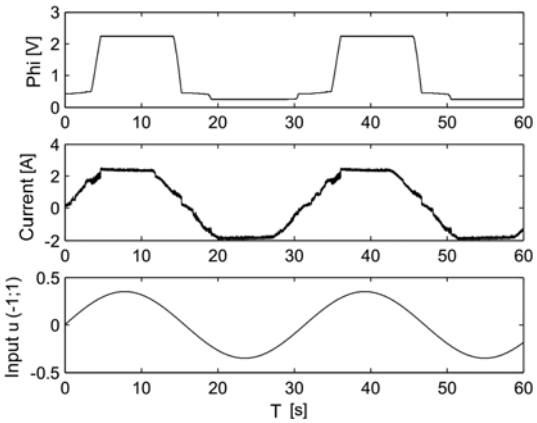


Figure 4. Response of the system subjected to a slow sinusoidal input (quasistatic) – time domain.

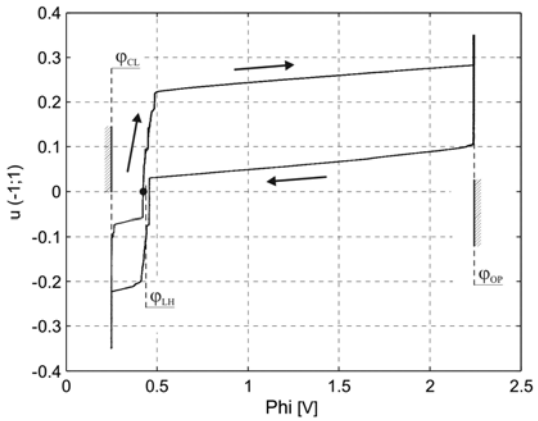


Figure 5. Response of the system subjected to slow sinusoidal input (quasistatic) – $\varphi$ vs. $u$ plot.

tion (hysteresis) of the system, c) the backlash in the LH position, and d) the high sensitivity to input in the opening operation range. The friction value can be easily estimated (in the interval [0,1]) along with the stiffness coefficients of the return spring. However, this data does not provide information about dynamic parameters (e.g., viscous damping and friction). The PE of the dynamic parameters requires faster changes of the input voltage, but the position must stay within rotation limits. This is difficult to guarantee with an open loop response; therefore, the approach described in Section 3.2 can be recommended as the next step of PE.

3.2. Parameter Estimation in Closed Loop Operation

For PE, the input–output set of behaviors while the plate position is inside its limits is needed. Contact with the limit ("bouncing") represents a very complex problem and must be excluded from the basic PE. The top parts of Figures 6 and 7 show data acquisition using a P controller with a relatively low gain. Figure 8 shows one typical system response. It can be seen that: a) the system does not fully follow the reference and b) the dry-friction properties are captured. Several samples of data were measured and used for the offline PE described in next two subsections.

3.2.1. PE using $u-\varphi_{SIM}$ data

The classical approach to PE would use a measured data pair, $u-\varphi_{SIM}$ (Figure 6). Here, the Nelder-Mead simplex search algorithm implemented in Matlab was used. Although many sets of numerical experiments were performed, the PE results were not satisfactory due to very high sensitivity to changes in the friction parameters.

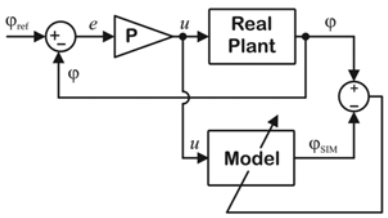


Figure 6. Block diagram of PE using input voltage, $u$, and output position, $\varphi_{SIM}$.

3.2.2. PE using $\varphi_{REF}-\varphi_{SIM}$ data

Comparatively better behavior was achieved using data pairs that included a low-gain P controller in the loop: $\varphi_{REF}-\varphi_{SIM}$ (see Figure 7). Due to dry friction, the system is relatively sensitive to small input variations (or imprecision), but the PE structure with a P controller effectively solves such problems. The input to the real plant and simulated one is different in this PE schema, but it can be proven that:

$$\begin{aligned} u-u_{SIM}&=k_P(\varphi-\varphi_{REF})-k_P(\varphi_{SIM}-\varphi_{REF})=k_P(\varphi-\varphi_{SIM})\\ u_{SIM}&=k_P(\varphi_{SIM}-\varphi_{REF})\\ u&=k_P(\varphi-\varphi_{REF}) \end{aligned} \tag{16}$$

Thus, the measure, $e=\varphi-\varphi_{REF}$, is sufficient for the evaluation of estimation quality. Figure 8 shows perfect correspondence between the measured and simulated data; Table 1 shows the values used.

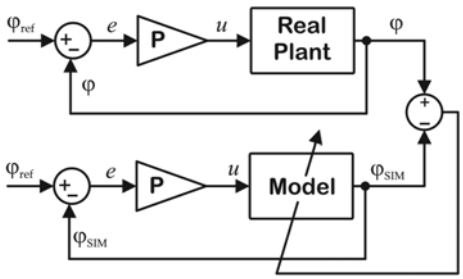


Figure 7. Block diagram of PE using input voltage, $\varphi_{REF}$, and output position, $\varphi_{SIM}$.

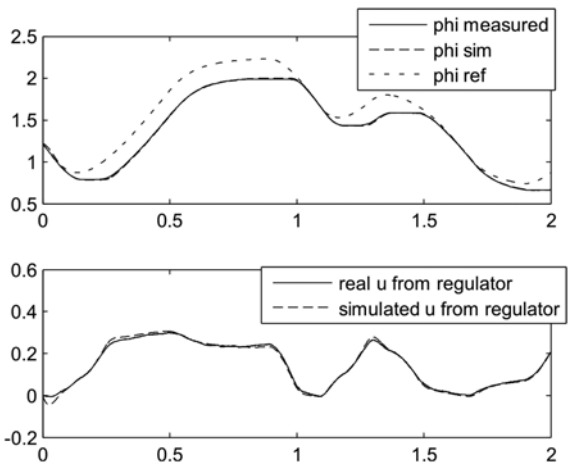


Figure 8. Top, an example of experimental data obtained in closed-loop that was further used for Parameter Estimation; Bottom, simulated data using estimated values.

Table 1. Estimated parameters using the Nelder-Mead method.

| Parameter | Estimated value |
|---|---|
| $u_{LH}$ | 0,1330 |
| $k_{OP}$ | 0,02079 |
| $u_{Fkin}$ | 0,06 |
| $u_{F\ stick}$ | 0,02 |
| J | 0,0004 |
| b | 0,025 |
| $\varphi_{LH}$ | 0,45 |
| $v_0$ | 0,1 |
| $\sigma_0$ | 200 |
| $\sigma_1$ | 0,01 |

## 4. NONLINEAR CONTROLLERS

### 4.1. Measuring Controller Performance Using Multiple Criteria

In this paper, several criteria were used to compare the performance of a controlled system. First, the standard Mean Square Error (MSE) was used and was characterized by strong weighting of large deviations:

$$MSE=\frac{1}{n}\sum_{i=1}^{n}(\varphi_{\mathrm{ref_i}}-\varphi_i)^2 \tag{17}$$

Further, the Mean Absolute Error (MAE) was used:

$$MAE=\frac{1}{n}\sum_{i=1}^{n}\left|\varphi_{\mathrm{ref_i}}-\varphi_i\right| \tag{18}$$

This measure emphasizes extreme values as much as the MSE and thus is often used as alternative.

Next, the Maximal Error (maxE) was used:

$$\max E=\max\left(\left|\varphi_{\mathrm{ref_i}}-\varphi_i\right|\right) \tag{19}$$

Determination of maxE is also important for the evaluation of controller quality.

Although previous criteria characterize the behavior of the controlled value satisfactorily, the behavior of the control action is not captured. Therefore, the activity of the control effort (CoEff) is also considered around the equilibrium value:

$$\mathrm{CoEf}=\frac{1}{n}\sum_{i=1}^{n}\left|u_i-u_{0_i}\right|$$
$$u_{0_i}=u_{\mathrm{spring_i}}+\mathrm{sign}(\dot{\varphi}_{\mathrm{ref}})u_{\mathrm{Fkin}} \tag{20}$$

Defined measures are used for a continuous reference signal. The staircase reference signal is considered only during a time interval of 0.2~0.5 sec (actual value modulo 0.5 sec.) because the settling time is about 0.15 sec. The CoEff uses a different equilibrium control effort:

$$u_{0_i}=u_{\mathrm{spring_i}}$$

### 4.2. Nonlinear Control Strategies

**PID** – This was the first controller tested, and the standard discrete implementation was used:

$$u_{\mathrm{PID}}=k_P(\varphi-\varphi_{\mathrm{ref}})+k_I\sum_{N}(\varphi-\varphi_{\mathrm{ref}})+u_{\mathrm{D}} \tag{21}$$

Derivative action is computed using an approach called the Derivative Impulse Area Invariant (Pivonka and Schmidt, 2007). The method is comparable to known Tustin approximations, but it provides slightly better results according to (Pivonka and Schmidt, 2007) and to our own experience. The discrete transfer function is of the following form:

$$u_{\mathrm{D}}(z)=\frac{T_{\mathrm{d}}}{T_{\mathrm{s}}}\left(1-e^{-\frac{GT_s}{T_{\mathrm{d}}}}\right)\frac{1-z^{-1}}{1-e^{-\frac{GT_s}{T_{\mathrm{d}}}}z^{-1}} \tag{22}$$

**Controller A –** In this strategy, PID is extended by feed-forward (FFC) spring compensation and feedback friction compensation based on position error (Isermann, 1996) (Figure 9):

$$u=u_{\mathrm{PID}}+u_{\mathrm{spring}}+u_{\mathrm{friction}}$$
$$u_{\mathrm{spring}}=f(\varphi_{\mathrm{ref}}-\varphi_{\mathrm{LH}}) \tag{23}$$
$$u_{\mathrm{friction}}=u_{\mathrm{F}}\ \mathrm{sign}(e^*),\quad e^*=\begin{cases} e-d, & \text{if } e>d \\ e+d, & \text{if } e<d \\ 0, & \text{else} \end{cases}$$

The dead zone used in the friction compensator significantly reduces chattering around the zero error position and thus improves controller properties.

**Controller B –** With this controller, PID and spring FFC are used as in variant A. The friction compensator is implemented by using the Smooth-Sliding Mode Control (SSMC) (Figure 10):

$$u=u_{\mathrm{PID}}+u_{\mathrm{spring}}+u_{\mathrm{SSMC}}$$
$$u_{\mathrm{spring}}=f(\varphi_{\mathrm{ref}}-\varphi_{\mathrm{LH}}) \tag{24}$$
$$u_{\mathrm{SSMC}}=u_{\mathrm{F}}\ \tanh(\alpha(\lambda e+\dot{e}))$$

A detailed description of SSMC and the settings of $\alpha$ and $\lambda$ can be found in (Young *et al.*, 1999).

**Controller C –** In this variant, the PID and spring FFC are implemented as in variant A. The friction compensator is implemented using SSMC combined with a simple position-error friction compensator that is switched off at every odd sample time. The compensator is shown in Figure 11 and is of following form:

$$u=u_{\mathrm{PID}}+u_{\mathrm{spring}}+u_{\mathrm{C}}$$
$$u_{\mathrm{C}}=\begin{cases} u_{\mathrm{SSMC}}, & |e|>e_S \\ u_F\ \mathrm{sign}(e)p(t) & \\ 0, & |e|<e_p \end{cases} \tag{25}$$

where $e_S$ and $e_p$ are the switching values obtained experimentally and $p(t)$ is a rectangular pulse signal with a period

of $2T_S$ and a duty factor 0,5.

**Controller D –** Here, the PID and spring FFC are implemented as in variant A. The friction compensator is identical to that in variant A (23) but is implemented as a feedforward. For the computation of discrete derivation is used Equation (22).

4.3. Implementation Details

4.3.1. Testing reference signal

Two types of position reference angle were used in our experiments: 1) a continuous reference signal that is a smooth signal simulates the slow change of required throttle position, and 2) a staircase reference signal that simulates the sudden change of plate angle. Both signals, shown in Figure 13, were generated randomly (except for the first part of the continuous signal). These signals were then stored and used in all experiments. Randomly generated signal is a good representation of variable driving conditions and covers virtually all possible changes of the reference.

4.3.2. Sample time and modeling of computational delay

Every practical design of ETC must address the limited computational power of low-cost microcontrollers used in cars. For each sample time, one must read the position of the throttle plate (i.e., ADC), compute an action using a given controller and set outputs (i.e., PWM, digital IO, or, for our case, DAC). The total time of these procedures, plus communication with the upper level of control, determines the minimal sample time. Figure 14 shows the timing schema on the microcontroller and the model used on

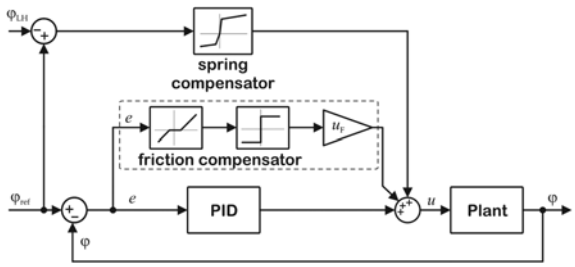


Figure 9. Block diagram of control with friction feedback compensation using position error (Controller A).

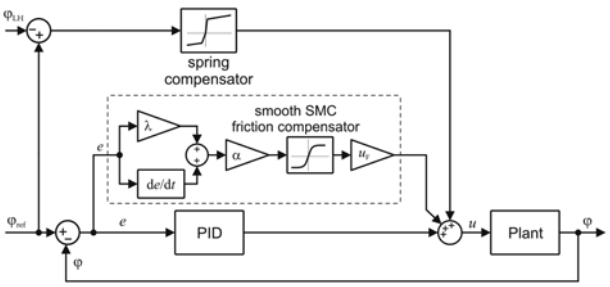


Figure 10. Block diagram of control with friction feedback compensation using SMC (Controller B).

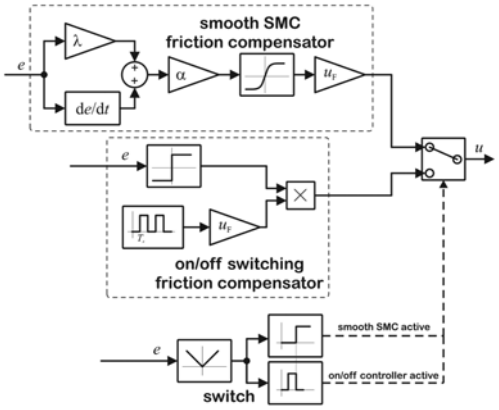


Figure 11. Block diagram of friction compensation using off-pulses near the zero error (Controller C).

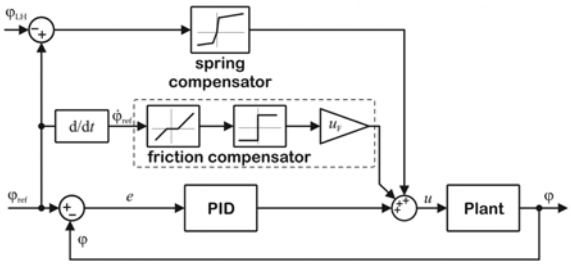


Figure 12. Block diagram of control with friction feedforward compensation (Controller D).

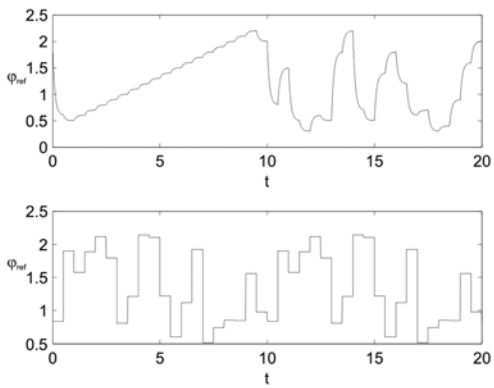


Figure 13. Continuous (smooth) and staircase reference angle signal used in all control experiments (see Table 2 and Table 3).

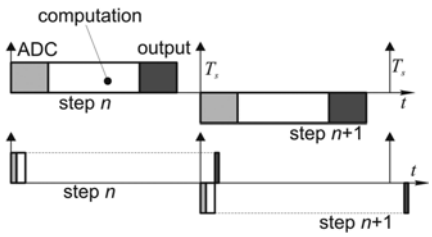


Figure 14. Timing on a real microcontroller (top) and a simulation of a microcontroller computational delay using RCP hardware from dSpace (bottom).

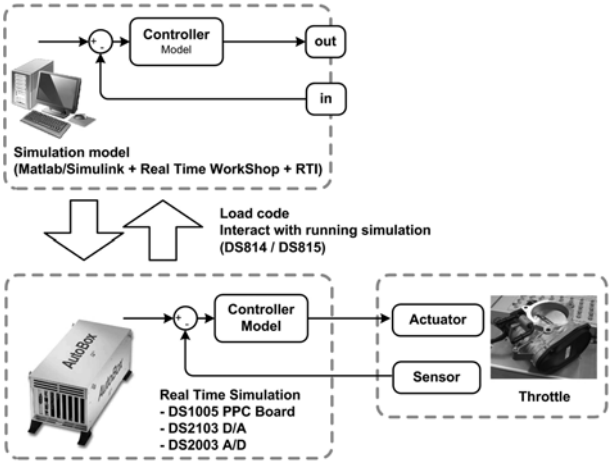


Figure 15. Schema of the RCP with dSpace modular hardware.

the RCP hardware. On the RCP hardware, computational time is very small. The goal is to simulate a delay similar to those seen in reality.

4.3.3. Hardware setup

The RCP-hardware used in our experimental setup is based on modular dSpace technology. It consists of a main processor (DS 1005 PPC), a board (DS 2103) with 14-bit D/A converters, a board (DS 2003) with 16-bit A/D converters, and communication cards (DS 814 and 815). RealTime Workshop in Simulink generates C-code for the DS 1005 PPC target, and the RTI (Real-Time Interface) provides a link between the code and the dSpace hardware. With a goal to minimize the hardware delay in the control loop, the operational power amplifier (SR4409439) from aPEX microTEX was used for the DC motor actuation. The physical measured voltage on the throttle potentiometer in the range of 0.25~2.25 V (2.25 V corresponds to full open) was used as the unit in this work. The input voltage, $u$, was normalized in the range $(-1;1)$.

4.1. Experimental Results

The controller structures described in Section 4.2 were tested using the two reference signals defined in Sec. 4.3.1.

Table 2. Multi-criteria evaluation of the controllers' behavior–continuous (smooth) reference signal.

| | Minimal sample time 50us | | | | Realistic sample time 5ms | | | |
|---|---|---|---|---|---|---|---|---|
| | MSE 1e-3 | MAE 1e-3 | maxE | CoEf 1e-3 | MSE 1e-3 | MAE 1e-3 | maxE | CoEf 1e-3 |
| PID | 0,103 | 4,18 | 0,175 | 75,5 | 0,698 | 14,2 | 0,252 | 101 |
| A | 0,108 | 3,43 | 0,165 | 84,4 | 1,08 | 13,5 | 0,308 | 66,6 |
| B | 0,404 | 6,76 | 0,212 | 65,5 | 0,878 | 13,6 | 0,272 | 75,3 |
| C | 0,119 | 4,28 | 0,168 | 80,6 | 0,902 | 13,7 | 0,292 | 74,5 |
| D | 0,119 | 4,30 | 0,169 | 44,6 | 0,835 | 12,6 | 0,290 | 43,1 |

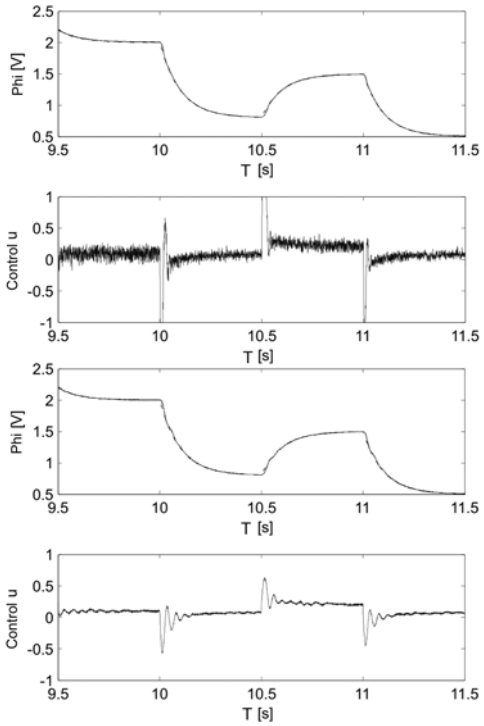


Figure 16. Responses using the continuous (smooth) reference. Sample time, 50us; PID controller (top) vs. Controller D.

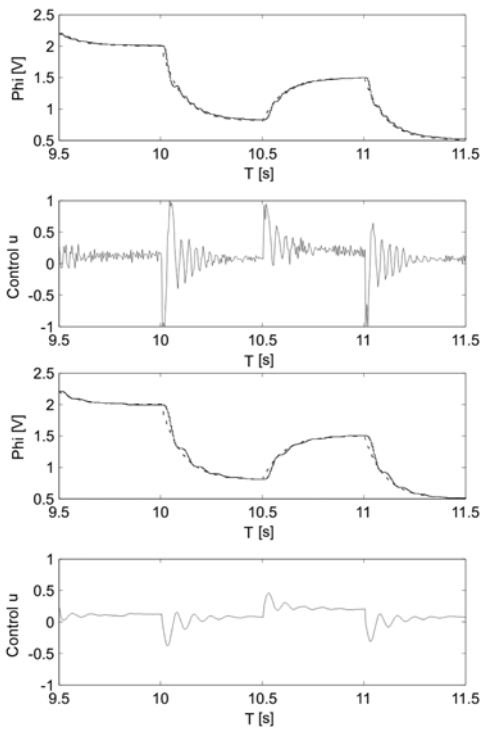


Figure 17. Responses using the continuous (smooth) reference. Sample time, 5 ms; PID (top) vs. Controller D.

Tables 2 and 3 summarize the results evaluated via the criteria introduced in Section 4.1. Figures 16~19 show the comparison of the system's response using PID and the

Table 3. Multi-criteria evaluation of the controllers' behavior–staircase reference signal.

| | Minimal sample time 50us | | | | Realistic sample time 5ms | | | |
|---|---|---|---|---|---|---|---|---|
| | MSE 1e-3 | MAE 1e-3 | maxE | CoEf 1e-3 | MSE 1e-3 | MAE 1e-3 | maxE | CoEf 1e-3 |
| PID | 0,414 | 14,6 | 0,0491 | 34,1 | 0,850 | 20,4 | 0,0849 | 40,4 |
| A | 0,00145 | 0,968 | 0,0049 | 79,5 | 0,0499 | 4,80 | 0,0299 | 20,2 |
| B | 0,00116 | 0,863 | 0,0039 | 70,4 | 0,0158 | 2,80 | 0,0150 | 44,4 |
| C | 0,00183 | 1,1 | 0,0053 | 0,660 | 0,00214 | 1,04 | 0,0089 | 15,5 |
| D | not working well | | | | not working well | | | |

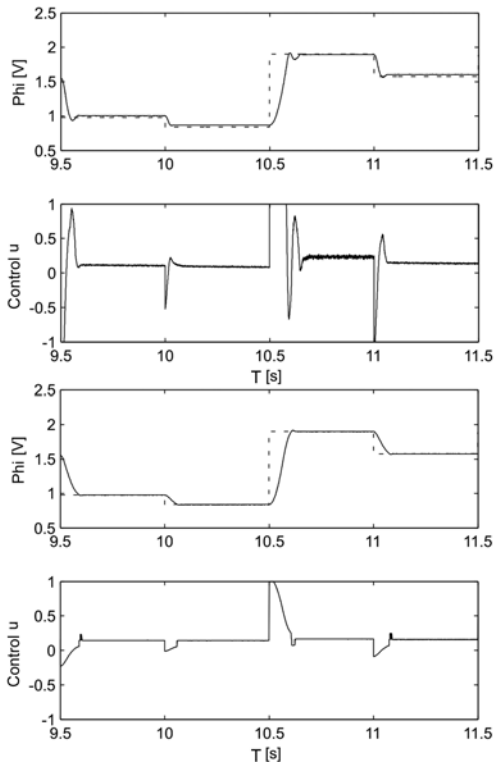


Figure 18. Responses using the staircase reference. Sample time, 50us; PID (top) vs. Controller C.

best candidate controller. Only two seconds (9.5~11.5 sec) are shown in detail, and the criteria in the Tables cover all experimental data (0~20 sec.).

A system with a smooth reference signal can be controlled using PID only, but the proportional gain is very high and can cause significant chattering (noise) around the target position (Figure 16). Controller D notably reduces the control effort (approx. 50%) given by CoEf and having similar MSE, MAE and maxE values. This result applies for both sample testing times (50 us vs. 5 ms).

The staircase reference signal disqualifies the PID from consideration, primarily in the realistic sample time of 5ms. This well-known disadvantage of using PID to control systems with high dry friction is fully visible here. Figure 19 (left) shows unacceptable steady state error. Also,

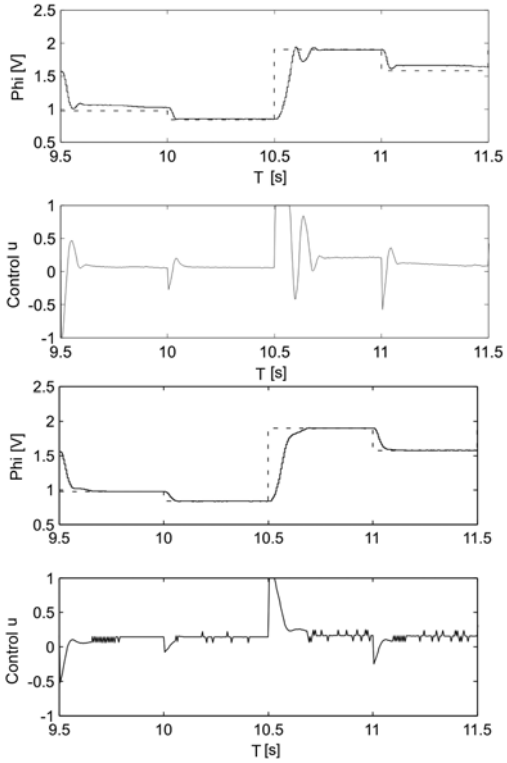


Figure 19. Responses using the staircase reference. Sample time, 5ms; PID (top) vs. Controller C.

Controller D does not work well in this case.

The staircase signal has either an infinite- or zero-derivative; thus, friction compensation in feedforward control cannot be used. Conversely, Controller C proves superior for control of the system. Table 3 summarizes the very good results given by this system, especially for the realistic sample time of 5 ms. The new controller feature, which switches off the action every even sample time near the target, significantly reduces the overcompensation and consequent oscillation around the reference.

## 5. CONCLUSION

Two new controller structures have been presented in this paper. The quality of the controllers has been measured using standard mean square error and by the consideration of required control effort, which has a direct influence on noise, vibration and wear of the throttle servo system. Compared with reports in previous publications, feedforward compensation for spring nonlinearity was used and has been verified as significantly more efficient. For the smooth reference signal, feedforward friction compensation is proposed along with the use of a derivative impulse-area invariant. For the staircase reference signal, an improved smooth sliding-mode controller was developed that switches off its activity every odd sample time, thus leading to an important decrease in control error and

control effort.

For practical applications, the implementation of a hybrid structure is recommended. In this case one of the two best candidates is switched on according to the derivative of the reference signal.

Two main steps for effective parameter estimation are also described. First, an open-loop quasistatic input signal is used to obtain the basic characteristics of the system. Then, a closed-loop scheme is used for the measurement of the system's dynamic response. Many experimental sets have been prepared, and the Nelder-Mead simplex search has been employed for offline parameter estimation.

All practical experiments were carried out using the Rapid Control Prototyping modular dSpace hardware.

**ACKNOWLEDGEMENT**–This work has been supported by the Automotive Mechatronics Parts Nurturing Group at Keimyung University, by the Ministry of Knowledge Economy (MKE) and Korea Institute of Industrial Technology Evaluation and Planning (ITEP) through the Center for Mechatronics Parts (CAMP) at Keimyung University and also by research project MSM 0021630518 "Simulation modelling of mechatronic systems".

## REFERENCES

Baotic, M., Vasak, M., Morari, M. and Peric, N. (2003). Hybrid system theory based optimal control of an electronic throttle. *American Control Conf.* 5209–5214.

Baric, M., Petrovic, I. and Peric, N. (2005). Neural network-based sliding mode control of electronic throttle. *Eng. App. Artificial Intelligence,* **18**, 951–961.

Beghi, A., Nardo, L. and Stevanato, M. (2006). Observer-based discrete-time sliding mode throttle control for drive-by-wire operation of a racing motorcycle engine. *IEEE Trans. Control Systems Technology,* **14**, 767–775.

Contreras, A. F., Quiroz, I. P. and Wit, C. C. (2002). Further results on modelling and identification of an electronic throttle body. *10th Mediterranean Conf. Control and Automation*, Lisbon, Portugal, July 9–12.

Deur, J., Pavkoviæ, D., Jansz, M. and Periæ, N. (2003). Automatic tuning of electronic throttle control strategy. *11th Mediterranean Conf. Control and Automation MED 2003*, Rhodes, Greece, June 18–20.

Grepl, R. and Lee, B. (2008a). Modelling, identification and control of electronic throttle using dSpace tools. *Technical Computing Prague 2008.*

Grepl, R. and Lee, B. (2008b) Modelling, identification and nonlinear control of electronic throttle. *In The KSAE Daegu Gyungbuk Regional Conf., Korean Society of Automotive Engineers. Daegu, Korea,* 45–53.

Hadilebbal, M., Chafouk, H., Hoblos, G. and Lefebvre, D. (2007). Modeling and identification of non-linear systems by a multimodel approach: application to a throttle valve. *Int. J. Information and Systems Sciences* **3**, **1**, 79–99.

Isermann, R. (1996). Information processing for mechatronic systems. *Robotics and Autonomous Systems,* **16**, 117–134.

Ishikawa, M., McCune, D., Saikalis, G. and Oho, S. (2007). CPU model-based hardware/software co-design, co-simulation and analysis technology for real-time embedded control systems. *13th IEEE Real Time and Embedded Technology and Applications Symp..*

Jung, H., Kwak, B. and Park, Y. (2000). Slip controller design for traction control system. *Int. J. Automotive Technology* **1**, **1**, 48–55.

Olsson, H., Åström, K. J., Canudas de Wit, C., Gäfvert, M., Lischinsky, P. (1998). Friction models and friction compensation, *Eur. J. Control* **4**, **3**, 176–195.

Pavković, D., Deur, J., Jansz, M. and Perić, N. (2006). Adaptive control of automotive electronic throttle. *Control Engineering Practice,* **14**, 121–136.

Pivonka, P. and Schmidt, M. (2007). Comparative analysis of discrete derivative implementations in PID controllers. *Systems Theory and Applications,* **2**, WSEAS, 33–37.

Ryu, J., Yoon, M. and Sunwoo, M. (2005). Development of a network-based traction control system, validation of its traction control algorithmand evaluation of its performance using net-hils. *Int. J. Automotive Technology* **6**, **2**, 171–181.

Stence, R. W. (2006). Digital by-wire replaces mechanical systems in cars, in electronic braking, traction, and stability controls. *Society of Automotive Engineers,* USA, 29–36.

Trebi-Ollennu, A. and Dolan, J. M. (2004). *Adaptive Fuzzy Throttle control for an All Terrain Vehicle, Institute for Complex Engineered Systems*. Carnegie Mellon University. Internal Report 04.

Young, K. D., Utkin, V. I. and Ozguner, U. (1999). A control engineer's guide to sliding mode control. *IEEE Trans. Control Systems Technology*, **7**, 1–14.

Vašak, M., Baotić, M., Petrović, I. and Perić, N. (2007). Hybrid theory-based time-optimal control of an electronic throttle. *IEEE Trans. Industrial Electronics*, **54**, 1483–1494.

Yang, C. (2004). Model-based analysis and tuning of electronic throttle controllers. *SAE World Cong.*, Detroit, Michigan, March 8–11.

Zhang, P., Yin, Ch. and Zhang, J. (2006). Sliding mode control with sensor fault tolerant for electronic throttle. *Int. Conf. Automation Science and Engineering, Shanghai*, China.